Path integrals in quantum mechanical systems

Author: Gerard Pons Polo
Facultat de Física, Universitat de Barcelona, Diagonal 645, 08028 Barcelona, Spain.

Advisors: Juan M. Torres and Assumpta Parreño
(Dated: June 13, 2023)

Abstract: This work has implemented the path integral formalism into quantum mechanics with systems at finite temperature. Low, medium and high temperatures have been considered. The study has been done with numerical computations based on Monte Carlo methods on the harmonic and the anharmonic oscillators. In this latter case the results have been compared with the Schrödinger equation solutions and it has lead to a high degree of compatibility. It has been shown that the path integral is an alternative and valid method to solve thermal quantum systems.

I. INTRODUCTION

The description of the world that surrounds us is one of the greatests aims of Physics, but often nature is complicated and unpredictable. Theories such as *Classical Mechanics* can explain scenarios which involve large objects and low velocities, but fail when trying to conceive the laws that govern our world at a smaller scale. Therefore, there is a need to create new physics in order to approach our perception of the world to the exact reality, in these cases where intuition can trick us. *Quantum Mechanics* introduces to physics the notion of probability and quantization. Well known properties of matter, such as energy and even the space position, are reconsidered at a low scale. This theory upholds that there are experiments from which one can not predict the final outcome. Quantum mechanical systems can have different states at the same time and these can be also modified by the observer while measuring it. This way of understanding the world, based just on probabilities and expected values of the outcomes, is what this theory stands for [1–3].

The system of this study is a particle in a one-dimensional potential. Two potentials will be treated, the harmonic and the anharmonic (in which a quartic interaction will be considered). The quantum harmonic oscillator has the following potential,

$$V(x) = \frac{1}{2} m\omega^2 x^2 \ , \tag{1}$$

and the anharmonic oscillator,

$$V(x) = \frac{1}{2} m\omega^2 x^2 + \frac{g^2}{2} x^4 \ . \tag{2}$$

The factor of quartic coupling g can take the following value for each potential: $g = 0$ for the harmonic oscillator (HO) and $g = 1$ for the anharmonic oscillator (AHO). These are only particular choices, the perturbative case would have $0 < g \ll 1$, and any other value would also work. For each potential, three system temperatures will be considered, $T = 10$, 1 and 0.1, in order to cover high, medium and low temperatures. The role of the temperature will be explained later on the developing sections.

The objective of this study is to develop a program that uses *path integrals* to study quantum mechanical systems at a finite temperature. Throughout this work, natural units will be used, and the parameters of the model will be set to one, without loss of generality. By choosing $m = 1$ the energy scale will be fixed, and the angular frequency dependence is not particularly interesting, so $\omega = 1$.

II. PATH INTEGRAL FORMALISM

Before the main formalism is presented, a few basics on classical physics serve as a starting point. Lets consider a one dimensional system with one particle in a potential. The principle of least action [4] allows to predict the most optimum trajectory by minimizing its action (S). The action of the system betwen a and b is defined as follows,

$$S = \int_{t_a}^{t_b} dt\, L(x, \dot{x}, t) \ , \tag{3}$$

where the Lagrangian (L) is,

$$L = \frac{m}{2}\dot{x}^2 - V(x, t) \ . \tag{4}$$

By considering the condition of extremum given by the least action principle, $\delta S = 0$, one can obtain the Euler-Lagrange equations,

$$\frac{d}{dt}\left(\frac{\partial L}{\partial \dot{x}}\right) - \frac{\partial L}{\partial x} = 0 \ . \tag{5}$$

The path integral formulation, created by Richard Phillips Feynman [2], arises from the desire of connecting both theories, classical and quantum mechanics, through the least action principle. Unlike *Classical Mechanics* that only considers one possible path for a particle going from a to b, *Quantum mechanics* contemplates all the infinite paths that the particle undertakes. This formulation allows to study these systems from a more precise

way by considering all these infinite paths [5]. Then, the probability of a particle that goes from a position x_a at a time t_a to a position x_b at a time t_b has to contemplate all the paths, and it is defined as $P(b;a) = K(b;a)$, where $K(b;a)$ is the transition amplitude from a to b, and it is constructed from all the possible paths, and each contribution has a phase proportional to the action S.

$$K(b;a) = K(x_b,t_b;x_a,t_a) = \sum_{\text{paths from } a \text{ to } b} A \cdot e^{i\frac{S}{\hbar}} \ . \quad (6)$$

Note that there is a constant A that normalizes K and whose value will be defined subsequently.

Now the paths need to be discretized [6], so the temporal interval will be divided into N steps of width ϵ. Then $t_b - t_a = N\epsilon$, with $t_0 = t_a$ and $t_N = t_b$. The discretized path can be expressed as $x(t) = (x_0, x_1, \dots, x_{N-1}, x_N)$, where each position of the path corresponds to its time step $x_i = x(t_i)$, and the boundary positions $x_0 = x_a = x(t_a)$ and $x_N = x_b = x(t_b)$ are fixed .

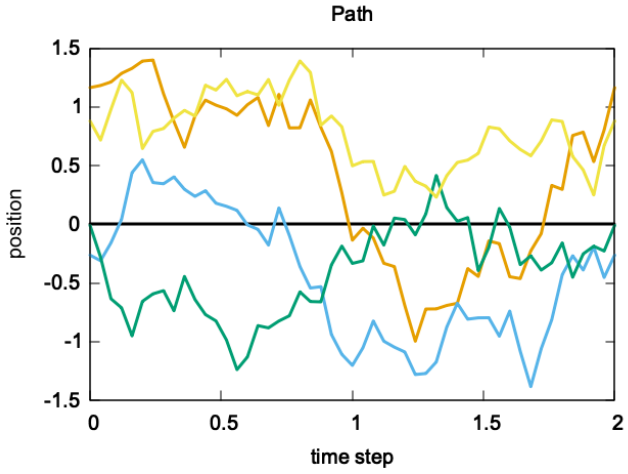

FIG. 1: Example of paths for the AHO with $g = 1$ and $T = 0.5$.

From here the sum over all paths can be expressed as an integral, in analogy with the *Riemann Integral*, by extending the sum to the limit $N \to \infty$ and $\epsilon \to 0$. Even though this limit does not exist in general, for our particular case, Eq. (4), it does and a *path integral* can be defined,

$$K(b;a) = K(x_b,t_b;x_a,t_a) = \int_{x(t_a)}^{x(t_b)} \mathcal{D}x(t)\, e^{i\frac{S}{\hbar}} \ , \quad (7)$$

where,

$$\mathcal{D}x(t) = \lim_{\epsilon\to 0} \frac{1}{A}\int \frac{dx_1}{A}\int \frac{dx_2}{A}\cdots\int \frac{dx_{N-1}}{A} = \\ = \left(\frac{m}{2\pi i\hbar\epsilon}\right)^{N/2} \prod_{i=1}^{N-1}\int dx_i \ , \quad (8)$$

and the normalization constant takes the form,

$$A = \left(\frac{2\pi i\hbar\epsilon}{m}\right)^{1/2} \ . \quad (9)$$

The action of a discretized path can be calculated by the approximation,

$$S[x(t)] = \sum_{i=0}^{N-1} S[x_{i+1}, x_i] \ . \quad (10)$$

Space (x) and velocity ($\dot{x}$) variables will take the following forms,

$$x_i \to \frac{x_{i+1}+x_i}{2} \ , \\ \dot{x_i} \to \frac{x_{i+1}-x_i}{\epsilon} \ . \quad (11)$$

Each contribution to Eq. (10), taking into account our Lagrangian (Eq. (4)), will end up resulting in

$$S[x_{i+1},x_i] = \int_{t_i}^{t_{i+1}} dt\, L\left(\frac{x_{i+1}+x_i}{2}, \frac{x_{i+1}-x_i}{\epsilon}\right) = \\ = \frac{m\epsilon}{2}\left(\frac{x_{i+1}-x_i}{\epsilon}\right)^2 - \epsilon\cdot V\left(\frac{x_{i+1}+x_i}{2}\right) \ . \quad (12)$$

Finite temperature

Here the temperature T is introduced to the formalism, allowing the study of thermal quantum systems and the final bases for the simulation to settle. We can express K as follows,

$$K(b;a) = \langle x_b | e^{i\frac{H(t_b-t_a)}{\hbar}} | x_a\rangle \ , \quad (13)$$

where H is the Hamiltonian of the system.
We will be interested in the diagonal elements of the transition amplitude. Therefore, we set the boundary limits to an equal value $x_0 = x_a = x_b$, and take $t_a = 0$ and $t_b = t$. Then, by introducing a complete set of states $\sum_n |n\rangle\langle n|$,

$$K(x_0,t;x_0,0) = \sum_n |\Psi_n(x)|^2 e^{i\frac{E_n t}{\hbar}} \ . \quad (14)$$

Comparing this expression with the definition of the partition function in thermodynamics,

$$\mathcal{Z} = \sum_n e^{-E_n\beta} \ , \quad (15)$$

or more precisely with the thermal density matrix, one can identify the relation between the time interval and the temperature,

$$\hbar\beta = it \ , \quad (16)$$

being $\beta = \frac{1}{k_B T}$, and k_B the Boltzmann constant that will take a value equal to one as long as natural units are used.

Given the oscillatory behaviour of the exponential in Eq. (14), not suited for numerical calculations, the time (t) is changed to an imaginary time (τ) by doing a Wick rotation, $t \to -i\tau$. Obtaining the expression that will be used from here on,

$$K(x_0, \beta; x_0, 0) = \int_{x_0 = x(0)}^{x_0 = x(\beta)} \mathcal{D}x(\tau)\, e^{-\frac{S_E}{\hbar}} \ , \tag{17}$$

where the Euclidean action (S_E) has been defined,

$$S_E[x(\tau)] = \sum_{i=0}^{N-1} \frac{m\Delta\tau}{2} \left(\frac{x_{i+1} - x_i}{\Delta\tau} \right)^2 + \Delta\tau \cdot V\left(\frac{x_{i+1} + x_i}{2} \right) \ , \tag{18}$$

with $\Delta\tau = \beta/N$.

III. METROPOLIS ALGORITHM

To simulate the *path integral* we will use the Metropolis algorithm. This algorithm is based on the Monte Carlo method and uses Markov chains [7]. There are a few steps to follow:

1. First an initial path is generated. It can be initialized with an arbitrary configuration, in this case: $x^0 = (0, \ldots, 0)$
2. Then a second path, based on the first one, is generated by adding a random number γ on a random position of the path: $x^1 = (0, \ldots, \gamma, \ldots, 0)$. This random number γ will be Gaussianly distributed, with a probability $N(\mu, \sigma)$ where $\mu = 0$ and σ to be decided.
3. From now on we calculate the actions of both paths using Eq. (18). The change of action is computed as $\Delta S = S^1 - S^0$.
4. Next, the new path has to be accepted or rejected according to the following criteria:
   - If the action of the new path is less than the original one, $\Delta S < 0$, the new path is accepted.
   - If the action of the new path is greater or equal than the original one, there is still a chance for the path of being accepted. In this case a random uniformly distributed number $\eta \in U[0, 1]$ is generated, and the new path will be acepted if $\eta < e^{-\Delta S}$. Otherwise the path is rejected, and an iteration ends.
5. Then the process is repeated from step (2) with the accepted path if it was accepted, or with the original path if the new one was rejected. The procedure continues until there is a significant number of accepted paths for the statistical computation.

Only the paths that are accepted will take part in the statistical computations. To avoid correlations, only one path out of N_c, with N_c a large enough number of paths, is used in the analysis.

This algorithm requires a thermalization period. To avoid fluctuations coming from the initialization of the iteration sequence, some paths need to be discarded, until a stabilization is reached and the paths are thermalized, as it is shown in the section *Action Thermalization* of the Appendix. Then, one of these paths initiates the algorithm and the collection of data for the study starts.

Adaptation of the method

Here a modification of the general Metropolis method is implemented. Notice that, the way this algorithm works, two consecutive paths are highly correlated, as long as they only differ on one point. A possible way to avoid this problem is, instead of generating the new path by taking the previous one and adding a random number on just one position, the new path can be generated by adding a random number on each position of the path. It is important to mention that boundary conditions will be also imposed, so the path begins and ends at the same place.

By implementing this substantial modification, the paths accepted are not correlated and allows us to make the statistical study with less iterations. However, the probability of accepting a new path is much smaller than the one obtained by changing a single point, therefore one needs to fix an appropriate value for σ, in this case by reducing it. The criterion to decide the value of σ is to fix it such that the path's acceptation rate of the Metropolis algorithm is $\simeq 50\%$.

Computation of physical properties

To compute any physical property, more tangible and measurable concepts than the action of the path need to be computed, such as the values of the position. To calculate the average value of any n power of the position, we can use the following equation,

$$\overline{x^n} = \langle x_i^n \rangle = \frac{\sum_j^{N_{\text{paths}}} x_j^n}{N_{\text{paths}}} \ , \tag{19}$$

where the index i makes reference to the position in each path and the j index runs over all accepted paths.
As long as each position of the path is equaly random, the averages values can be calculated with any of the path position x_i, so its index will be suppressed for a simpler notation.

This value has an statistical uncertainty because the number of paths will never be infinite, so the error associated goes as $\frac{1}{\sqrt{N_{\text{paths}}}}$ according to [8],

$$\delta_{\langle x^n \rangle} = \sqrt{\frac{\langle x^{2n} \rangle - \langle x^n \rangle^2}{N_{\text{paths}}}} \ . \tag{20}$$

IV. RESULTS

Here the final results are presented. First the implementation of the temperature is discussed. A few comparisons will be given for the probability distributions resulting from the path integral simulations $P(x)$.

We will start with the HO. This potential has a well-known solution for any temperature. The probability distribution for this potential is [3],

$$P_{HO}(x) = \sqrt{\frac{\tanh\left(\frac{\beta}{2}\right)}{\pi}} e^{-x^2 \tanh\left(\frac{\beta}{2}\right)} \ , \tag{21}$$

for the parameters we have chosen ($\omega = m = 1$).
In Fig. 2 the harmonic oscillator distributions $P(x)$ obtained from the path integral simulations (MC), are compared with their respective theorical probability functions (TH), for the three temperatures. As T increases, the distribution gets broader due to the thermal fluctuations.

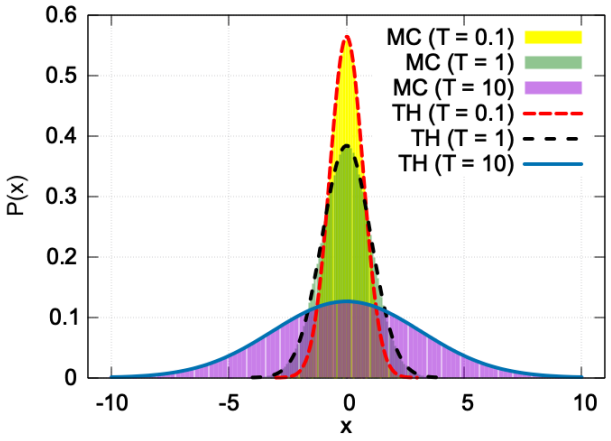

FIG. 2: Probability distributions of x for the harmonic oscillator $P(x)$, for the three temperatures. The corresponding theoretical probabilities given in Eq. (21) are also represented.

Next, in order to study the correctness of the Monte Carlo method in a case without analytic solution, as it is the anharmonic oscillator, the distribution computed with the path integral simulations (MC) will be compared with the probability distribution obtained directly from the simulation of the Schrödinger equation ($P_S(x)$) [9]. Fig. (3) shows that the probabilities computed with the path integral are compatible with the Schrödinger probability distributions.

To optimize the data collection, the program has run with different parameters for each temperature. The values can be found at the section *Program parameters* of the Appendix.

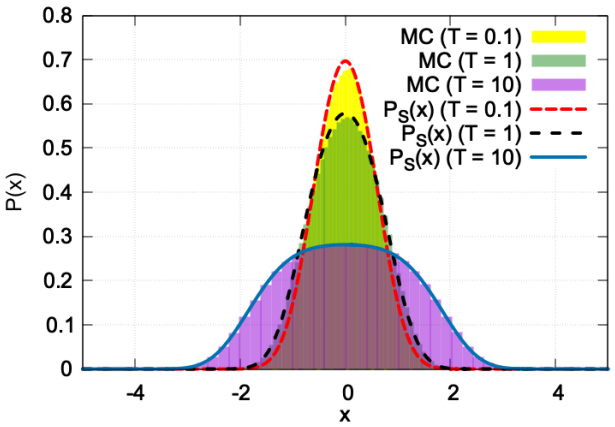

FIG. 3: Distribution of x for the anharmonic oscillator (AHO) for $g = 1$, considering the three temperatures. The corresponding Schrödinger probabilities $P_S(x)$ are also represented.

After the analysis of the temperature dependence of the probability distribution, a comparison of the energies of the system will be discussed. To compute the energies of the ground states we use the *virial theorem*,

$$2\langle T \rangle = \left\langle x \frac{dV(x)}{dx} \right\rangle \ . \tag{22}$$

As $H = T + V$, and considering Eq. (2) (with $m = \omega = 1$), this leads to,

$$\langle E \rangle = \langle x^2 \rangle + \frac{3}{2} g^2 \langle x^4 \rangle \ , \tag{23}$$

with the associated uncertainty,

$$\delta_E = \delta_{\langle x^2 \rangle} + \frac{3}{2} g^2 \delta_{\langle x^4 \rangle} \ . \tag{24}$$

The results used to compute the energies $\langle E \rangle$ can be found at the section *Expected values* of the Appendix. For the harmonic oscillator, the energies are compared with the theoretical ones, that can be obtained with the expected values of $\langle x^2 \rangle$ and $\langle x^4 \rangle$, which, as long as the analytical expression of the probability distribution is known, can be calculated as,

$$\langle x^n \rangle = \int_{-\infty}^{\infty} P(x) x^n dx \ , \tag{25}$$

where,

$$P(x) = \frac{K(x,\beta;x,0)}{\int_{-\infty}^{\infty} K(x,\beta;x,0)dx} \ . \tag{26}$$

For the anharmonic oscillator the energies are compared with the ones obtained by solving the Schrödinger equation and computing the value of the probability using the corresponding eigenvalues and eigenfunctions in Eq. (14) after doing a Wick rotation ($t \to -i\tau$).
In Table I we can see that the energies calculated from the path integral simulations are quite similar with their respective comparations.

TABLE I: Average energy $\langle E \rangle$ of the systems (HO, AHO) for three different temperatures.

Temperature	$\langle E \rangle$	
	Numerical	Exact, from Eq.(21)
$T = 0.1$	0.5084 ± 0.0003	0.500
$T = 1$	1.0927 ± 0.0002	1.082
$T = 10$	10.0232 ± 0.0006	10.008

(a) Harmonic Oscillator

Temperature	$\langle E \rangle$	
	Numerical	Schrödinger
$T = 0.1$	0.7358 ± 0.0009	0.696
$T = 1$	1.0522 ± 0.0004	1.050
$T = 10$	7.9380 ± 0.0007	7.905

(b) Anharmonic Oscillator

V. CONCLUSIONS

This work has proved the Path Integral formulation to be a robust method for the study of thermal quantum systems. It has resulted to be an elegant way of connecting the world of Quantum Mechanics with the classical concepts via computational Monte Carlo simulations.

The results obtained follow the expected behaviour with a reasonable accuracy, and can be summarized as:

- The simulation is based on Monte Carlo methods, so statistical uncertainties can be drasticaly reduced by increasing the number of paths used in the simulation. The only inconvenient is the longer computation times.

- For the harmonic oscillator the histograms obtained for the x distribution agree with the theoretical probability distribution. In addition, as the temperature increases the distribution widens, since the energy of the particle increases as the temperature increases, and this allows the particle to reach higher levels of energy where it can travel longer distances away from the equilibrium point.

- For the anharmonic oscillator, the distribution does not have any analytical expression to compare with, but they agree really well with the Schrödinger calculation, in particular for low temperatures where the quantic effects are more relevant. We shall mention that there is small discrepancy due to some systematic error.

The project has allowed integrating *Quantum Mechanics* and *Computational Physics* in order to develop a powerful and dynamic program which is very versatile and easily extrapolable to other systems with different potentials and space dimentions. It has also contributed to consolidate the skills of multidisciplinary work as well as taking some of the basics learnt during the degree to another level.

Acknowledgments

I would like to thank my advisors Juan M. Torres and Assumpta Parreño for the excellent guiding of this final degree project, and also thanks to Álvaro Peña Almazán for the contribution of the Schrödinger equation data on the comparison of the anharmonic potential.

[1] Dirac, Paul Adrien Maurice, (1930), *The Principles of Quantum Mechanics*, Oxford: Clarendon Press
[2] Feynman, Richard Phillips and Leighton, Robert B. and Sands, Matthew Linzee (1964), *The Feynman Lectures on Physics*, volume 3, Addison-Wesley, Redwood City, CA
[3] Feynman, Richard P and Hibbs, Albert R and Styer, Daniel F, (2010), *Quantum mechanics and path integrals*, Courier Corporation
[4] N. S. Manton, (2013), *The Principle of Least Action in Dynamics*, DAMTP, Centre for Mathematical Sciences, Wilberforce Road, Cambridge CB3 0WA, UK.
[5] R. Rosenfelder, (2017), *Path Integrals in Quantum Physics*, [arXiv:1209.1315 [nucl-th]]
[6] Daniel Elebiary, (2020), *Path Integral Simulation of the Harmonic and Anharmonic Oscillators*, Treball de Final de Grau, UB, [http://hdl.handle.net/2445/176475]
[7] G. P. Lepage, (2005), *Lattice QCD for Novices*, [arXiv:hep-lat/0506036]
[8] R. J. Serfling, (1980), *Approximation Theorems of Mathematical Statistics*, JOHN WILEY & SONS, INC.
[9] Álvaro Peña Almazán, (2023), private communication

Appendix

Action Thermalization

In order to study the thermalization of the algorithm, the action of each accepted path as a function of the number of accepted paths will be represented. By increasing the number of paths the action reaches its expected value and then stabilizes. For different temperatures, the thermalization period is achieved with a different number of accepted paths.

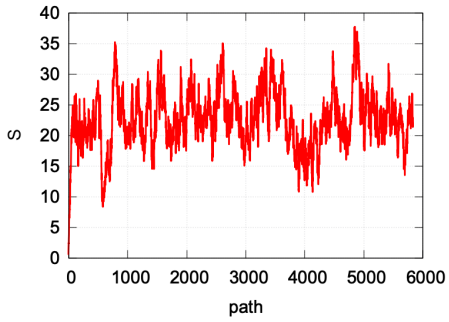

(a) $T = 0.1$

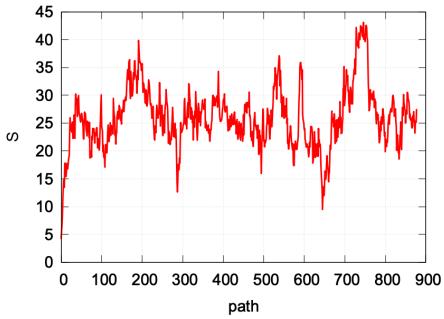

(b) $T = 1$

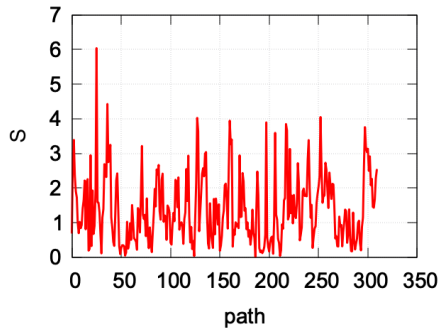

(c) $T = 10$

FIG. 4: Thermalization of the action for the harmonic oscillator for three different temperatures.

Fig. 4 shows that as temperature increases the action of the system stabilizes with a smaller number of paths, due to the thermal fluctuations.
In this work the number of paths for the thermalization period, required in the algorithm, has been set to 10^6 paths, in order to cover any possible temperature dependence, especially at lower temperatures where a larger number of paths is required to thermalize.

Program parameters

The parameters used in the simulation, such as the number of steps for the paths discretization (N) or the number of iterations for the algorithm, are the ones shown in Table II.

TABLE II: Values used in the simulations for each temperature. Runtimes are also indicated.

Temperature	***N***	**Iterations**	**Runtime**
0.1	50	10^7	30 s
1	20	10^8	2.5 min
10	5	10^9	12 min

Expected values

Here the expected values of x are tabulated, for each potential and temperature. These results have been acquired using Eq. (19). The harmonic oscillator is compared with the values directly calculated using the analytical solution, Eq. (21), as input of Eq. (25).
The anharmonic oscillator is compared with the values calculated from the solution of the eigenvalues and eigenfunctions of the Schrödinger equation into Eq. (14) after a Wick rotation is performed and then, into Eq. (25). Remember that $P(x;\beta = \frac{1}{T}) = K(x,\beta;x,0)$. These results are the ones that have been used in the calculation of the energies $\langle E \rangle$.

TABLE III: Average value of different powers of the position, $\langle x^n \rangle$ $n \in \{1,2,3,4\}$, for a system temperature $T = 10$.

Harmonic Oscillator		
$\langle x^n \rangle$	*Numerical*	*Theoretical*
$\langle x \rangle$	$(3.14 \pm 0.01) \cdot 10^{-2}$	0
$\langle x^2 \rangle$	10.0232 ± 0.0006	10
$\langle x^3 \rangle$	0.640 ± 0.005	0
$\langle x^4 \rangle$	300.09 ± 0.04	300
Anharmonic Oscillator		
$\langle x^n \rangle$	*Numerical*	*Schrödinger*
$\langle x \rangle$	$(4.29 \pm 0.05) \cdot 10^{-3}$	0
$\langle x^2 \rangle$	1.39032 ± 0.00007	1.386
$\langle x^3 \rangle$	$(1.22 \pm 0.02) \cdot 10^{-2}$	0
$\langle x^4 \rangle$	4.3651 ± 0.0004	4.345

TABLE IV: Average value of different powers of the position, $\langle x^n \rangle$ $n \in \{1, 2, 3, 4\}$, for a system temperature $T = 1$.

Harmonic Oscillator		
$\langle x^n \rangle$	*Numerical*	*Theoretical*
$\langle x \rangle$	$(-1.40 \pm 0.01) \cdot 10^{-2}$	0
$\langle x^2 \rangle$	1.0927 ± 0.0002	1.082
$\langle x^3 \rangle$	$(-6.34 \pm 0.06) \cdot 10^{-2}$	0
$\langle x^4 \rangle$	3.6019 ± 0.002	3.512
Anharmonic Oscillator		
$\langle x^n \rangle$	*Numerical*	*Schrödinger*
$\langle x \rangle$	$(1.415 \pm 0.009) \cdot 10^{-2}$	0
$\langle x^2 \rangle$	0.42019 ± 0.00008	0.406
$\langle x^3 \rangle$	$(1.25 \pm 0.01) \cdot 10^{-2}$	0
$\langle x^4 \rangle$	0.4563 ± 0.0002	0.429

TABLE V: Average value of different powers of the position, $\langle x^n \rangle$ $n \in \{1, 2, 3, 4\}$, for a system temperature $T = 0.1$.

Harmonic Oscillator		
$\langle x^n \rangle$	*Numerical*	*Theoretical*
$\langle x \rangle$	$(-5.0 \pm 0.3) \cdot 10^{-3}$	0
$\langle x^2 \rangle$	0.5084 ± 0.0003	0.5
$\langle x^3 \rangle$	$(-2.53 \pm 0.06) \cdot 10^{-2}$	0
$\langle x^4 \rangle$	0.789 ± 0.001	0.75
Anharmonic Oscillator		
$\langle x^n \rangle$	*Numerical*	*Schrödinger*
$\langle x \rangle$	$(6 \pm 3)10^{-4}$	0
$\langle x^2 \rangle$	0.3179 ± 0.0002	0.306
$\langle x^3 \rangle$	$(-6 \pm 3)10^{-4}$	0
$\langle x^4 \rangle$	0.2786 ± 0.0004	0.260